2-D Beam-Steerable Generalized Mikaelian Lens With Unique Flat-Shape Characteristic

Wenyi Shao, *Student Member, IEEE*, and Qiang Chen, *Senior Member, IEEE*

***Abstract*—A novel two-dimensional (2-D) beam-steerable generalized Mikaelian lens is presented in this letter. The main difference of proposed lens with respect to conventional Luneburg, Maxwell fish-eye and Eaton lens is its unique flat-shape characteristic, which provides great advantages in designing the low-profile flat-shape lens antenna, avoiding using extremely complex conformal mapping methods. The all-dielectric low-cost lens prototype presenting desired graded permittivity profile is fabricated by 3-D printing. The measurement results at 10 GHz show 2-D beam-steering capabilities from −20° to 20° in both the *E*-and *H*-plane with around 18.9 dBi of realized gain with less than ∼1.2 dB variation and low-side lobe can be achieved, revealing great potentials for developing the low-profile and cost-effective lens antenna for microwave applications.**

***Index Terms*—3-D printing, beam steering, gradient-index, lens antenna, Mikaelian lens.**

I. Introduction

GRADIENT index (GRIN) lens has attracted significant interest for its attractive properties, such as broadband, high directivity, competitive efficiency, and ease of fabrication, in microwave and millimeter-wave applications. Unlike electronically phased array and bulky mechanically steerable reflector, GRIN lens can flexibly achieve wide beam-steering angles with less deterioration of the beam. There have been several well-known GRIN lenses, such as Luneburg lens [1], Maxwell fisheye lens [2], and Eaton lens [3]. Although these lenses have various refractive index profiles defined under different spatial coordinates, a common feature among them is the spherical nature of their shapes that poses a significant manufacturing challenge. To overcome such limitations, a more convenient approach is to use extremely complex transformation optics (TO) [4] or quasi-conformal transformation optics (QCTO) [5] method to design flat-shaped lens (e.g., planar Luneburg lens) while maintaining the original electromagnetic performances.

However, a self-focusing cylindrical lens structure called Mikaelian lens [6] has not been exhaustively reported in the literature of microwave applications. The main difference of Mikaelian lens with respect to the Luneburg, Maxwell fish-eye and Eaton lens is its unique flat-shape characteristic and cylindrical symmetry of its refractive index profile [7] as shown in Fig. 1,

Manuscript received July 3, 2021; revised July 29, 2021; accepted August 1, 2021. Date of publication August 6, 2021; date of current version October 6, 2021. *(Corresponding author: Wenyi Shao.)*

The authors are with the Department of Communications Engineering, Tohoku University, Sendai 980-8579, Japan (e-mail: shao-w@ecei.tohoku.ac.jp; chenq@ecei.tohoku.ac.jp).

Digital Object Identifier 10.1109/LAWP.2021.3102316

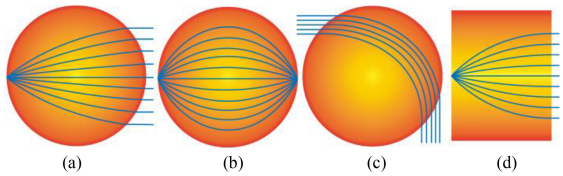

Fig. 1. Unique intrinsic flat-shape characteristic of Mikaelian lens. (a) Typical Luneburg lens. (b) Maxwell fish-eye. (c) Eaton lens. (d) Typical Mikaelian lens.

which make it very flexible and simple to fabricate. Moreover, it has the property of being spherical aberrations free like Luneburg lens, and is therefore an excellent candidate for focusing and beam steering. Most importantly, this lens concept has intrinsic low profile characteristic. Extra methods or techniques such as TO and QCTO are not required to flatten the particular shape. The focal length can be also easily determined by selecting the appropriate gradient parameter of refractive index profile of lens for different configuration scenarios. Although different manufacturing methods such as drilling holes [8], meta-surfaces [9], and pressing foam [10] were reported, all these previous studies mainly focused on the typical case with blocky structure that the source feed can only be placed on the lens surface, as shown in Fig. 1(d). Meanwhile, the beam-steering ability of Mikaelian lens concept has also not been investigated or mentioned.

In this letter, we introduce a generalized Mikaelian Lens using perforated dielectric for beam-steering application. Compared with the typical Mikaelian lens, it is much thinner, and has greater design freedom for different antenna configuration scenarios. It can also achieve two-dimensional (2-D) beam steering in both planes while keeping a low flat-shape profile, which provides a potential alternative to the existing planar GRIN lens antenna configurations based on complex conformal mapping methods. By using full-wave simulation, the focusing properties and performances of generalized Mikaelian lens are analyzed and validated from 8.5 to 12 GHz.

II. Mikaelian Lens Design

A. Design Theory of Mikaelian Lens Based on Ray Transfer Matrices

Mikaelian lens has a unique self-focusing property that the rays oscillate in a sinusoidal way inside lens, as shown in Fig. 2(a). The oscillation period of the rays is defined as pitch (p). Obviously, the different effects such as focusing, collimation, and diverging can be achieved by simply adjusting the pitch

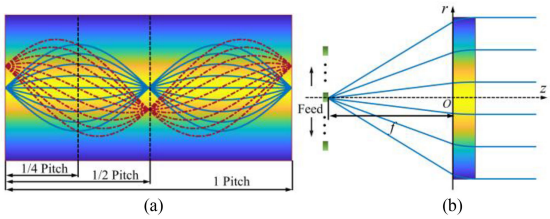

Fig. 2. Unique self-focusing properties of Mikaelian lens. (a) Rays oscillate in a sinusoidal way inside lens. (b) Schematic of off-body generalized Mikaelian lens antenna.

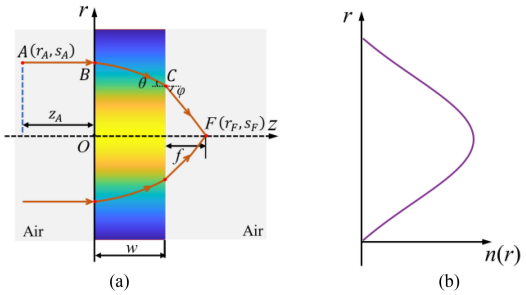

Fig. 3. (a) Rays through the Mikaelian lens. (b) Transverse refractive index profile of Mikaelian lens.

and thickness of lens. This characteristic allows for greater flexibility to design different antenna configuration scenarios such as off-body fed lens antenna, as shown in Fig. 2(b).

The transverse refractive index profile of generalized Mikaelian lens is defined by the following equation:

$$n(r) = n_0 \mathrm{sech}(2\pi p r/w) \tag{1}$$

where w is the thickness of lens. n_0 is the central refractive index along the z-axis. Particularly, when $p = 1/4$, (1) can be reduced to the typical form in [9], [10].

In our case, the ray traveling parallel to z-axis incident on the front surface of lens, and finally intersect at a point F, as shown in Fig. 3(a).

The ray behavior inside lens can be described by its distance (r_i) from the optical axis (z-axis) and by the slope (s_i) in any plane perpendicular to z-axis. i represents the different points in ray trajectory. For simplicity, $\alpha = 2\pi p/w$. n_{air} is refractive index of air. After propagating through the H-S lens, the ray refracts obeying Snell's law, and finally intersect at a point (F). Then, the ray trajectory from initial point A to focal point F can be obtained by using 2-by-2 ray transfer matrices [11].

$$\begin{aligned}\begin{pmatrix} r_F \\ s_F \end{pmatrix} &= \begin{pmatrix} 1 & f \\ 0 & 1 \end{pmatrix} \cdot \begin{pmatrix} 1 & 0 \\ 0 & n(r_C)/n_{air} \end{pmatrix} \\ &\cdot \begin{pmatrix} \cos(\alpha z) & \frac{\sin(\alpha z)}{\alpha} \\ -\alpha \sin(\alpha z) & \cos(\alpha z) \end{pmatrix} \cdot \begin{pmatrix} 1 & 0 \\ 0 & n_{air}/n(r_B) \end{pmatrix} \\ &\cdot \begin{pmatrix} 1 & z_A \\ 0 & 1 \end{pmatrix} \cdot \begin{pmatrix} r_A \\ s_A \end{pmatrix} \end{aligned} \tag{2}$$

Under the paraxial approximation [12], (2) can be further simplified as follows

$$f = w/(2\pi p n_0) \cdot \cot(2\pi p) \tag{3}$$

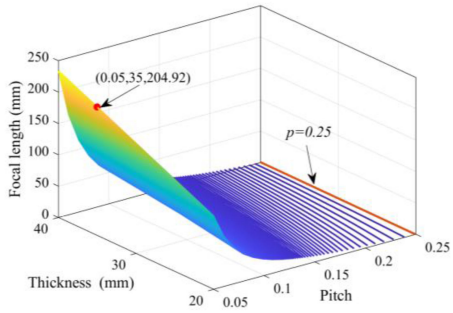

Fig. 4. Flexible design constraint of proposed Mikaelian lens.

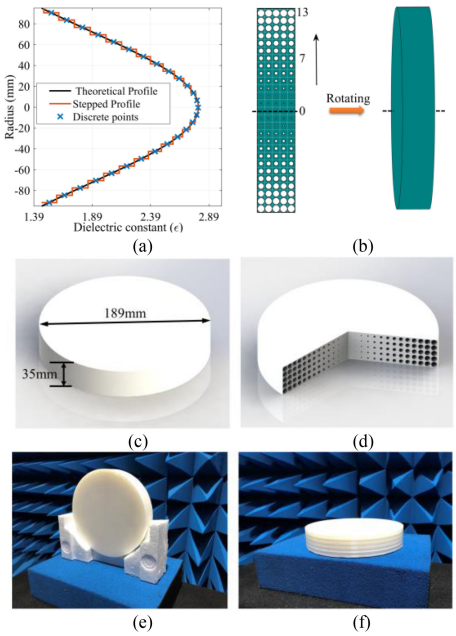

Fig. 5. Specific design procedure of proposed Mikaelian lens operating at 10 GHz. (a) Discretization of continuous relative permittivity profile by staircase approximation. (b) Rotating operation of 2-D perforated dielectric lens structure. (c) 3-D model of lens. (d) Cross section of designed lens model. (e) and (f) Photograph of the fabricated lens prototype.

Obviously, (3) provides a flexible design constraint of Mikaelian lens for different antenna configuration scenarios, as illustrated in Fig. 4. The most suitable thickness and focal length of lens can be easily chosen by simply adjusting pitch, according to Fig. 4. The red orange line represents $p = 0.25$. Under this condition, the focal length is equal to zero that means rays converge and focus at the rear surface of lens as abovementioned typical Mikaelian lens structure. The red point represents the specific design parameter ($p = 0.05$, $w = 35$ mm, $f = 204.92$ mm) of designed Mikaelian lens in our case.

B. Proposed Mikaelian Lens With Perforated Structure

Fig. 5 illustrates the specific design procedure of proposed Mikaelian lens operating at 10 GHz. The continuous relative permittivity profile of lens needs to be discretized by staircase approximation as shown in Fig. 5(a). In order to achieve the stepped relative permittivity profiles of lens, the perforated structure with different hole sizes is utilized. Owing to the axial

TABLE I
SPECIFIC DESIGNED HOLE SIZES FROM LAYER 0 TO 13

Layer	Diameter of holes
0	0.316 mm
1	0.653 mm
2	1.226 mm
3	1.816 mm
4	2.399 mm
5	2.968 mm
6	3.517 mm
7	4.042 mm
8	4.542 mm
9	5.013 mm
10	5.456 mm
11	5.870 mm
12	6.253 mm
13	6.608 mm

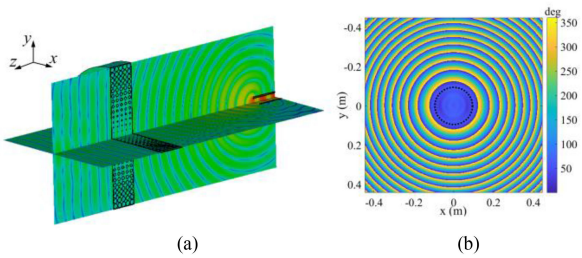

(a) (b)

Fig. 6. Focusing performances of proposed Mikaelian lens. (a) Simulated 2-D electric field distribution at *xoz* and *yoz* plane with WR-90 waveguide as source feed. (b) Aperture phase distribution at a plane located at the exit aperture of Mikaelian lens. The black dot circle represents the actual physical aperture (0.189 m diameter) of lens.

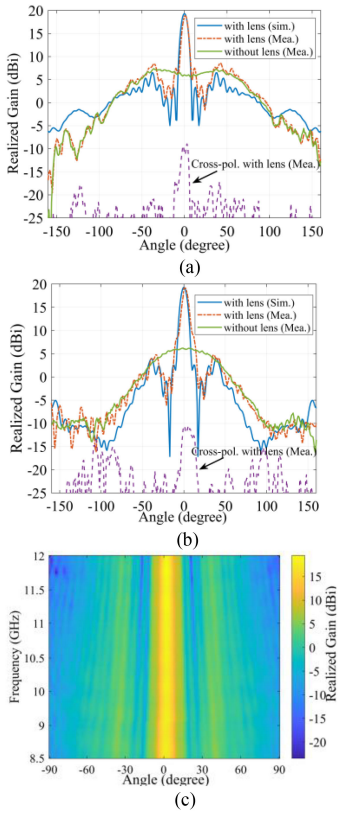

Fig. 7. Simulated and measured radiation patterns of the proposed Mikaelian lens antenna at 10 GHz. (a) *E*-plane. (b) *H*-plane. (c) Measured realized gain in the *H*-plane as a function of the frequency.

symmetry of lens, Table I only lists the specific hole sizes from layer 0 to 13.

The 3-D model of lens can be created by rotating the discrete 2-D perforated structure around the central axis, as shown in Fig. 5(b). It is easy and low-cost to be fabricated by using fused deposition modeling (FDM) 3-D printing. The polylactic acid (PLA) plastic material is utilized to fabricate proposed Mikaelian lens, which has a relative dielectric constant $\varepsilon_{\mathrm{PLA}} \approx 2.75$, and loss tangent $tan\delta \approx 0.011$. Here, the cross section of 3-D lens model is shown in Fig. 5(c) and (d), which has circular geometry with the diameter of 189 mm and the thickness of 35 mm. The designed focal length is 204.9 mm, and the focal length to lens diameter ratio (f/D) is 1.08.

III. NUMERICAL VERIFICATION AND MEASUREMENT RESULTS

A. Focusing Performances

To illustrate the focusing performance, the proposed Mikaelian lens model is constructed and simulated using the electromagnetic field full-wave simulation in CST Microwave Studio. Fig. 6(a) shows the 2-D electric field distribution propagating through the lens at *xoz* and *yoz* plane with WR-90 waveguide as source feed, which demonstrates very good focusing performances of Mikaelian lens. The aperture phase distribution is nearly uniform across the exit aperture plane of lens as shown in Fig. 6(b), which further illustrate the good phase transformation function (spherical wave to plane wave) of lens. It is to be noted that the black dot circle represents the actual physical aperture (0.189 m diameter) of lens.

Fig. 7(a) and (b) shows the simulated and measured radiation patterns for the WR-90 waveguide with and without the presence of the lens, for both the *E*-plane (*yoz* plane) and *H*-plane (*xoz* plane). The measured realized gain of the waveguide is about 5.8 dBi, and the realized gain of the lens antenna is about 18.9 dBi that is 13.1 dBi higher than the feed itself. It demonstrates the high realized gain can be achieved owing to the good phase transformation function of lens. Furthermore, the measured cross-polar levels of both *E*- and *H*-planes remain at a low level (less than –28 dB). The measured realized gain in the *H*-plane is only plotted as a function of the frequency for brevity, which demonstrates the broadband behavior of the proposed lens, as shown in Fig. 7(c).

B. 2-D Beam-Steering Capability

The waveguide is placed at the focal plane of the lens, and can be moved in *x*-and *y*-axis as shown in Figs. 8 (a) and 9(a), respectively. Fig. 8(b) shows one examples of simulated 2-D electric field distribution for feeding position (x $= -30$ mm). It indicates that the waveguide placed at off-center position of lens leads to a steered beam. Considering the symmetric structure of lens, symmetric radiation patterns can be obtained for the corresponding symmetric feed positions with respect

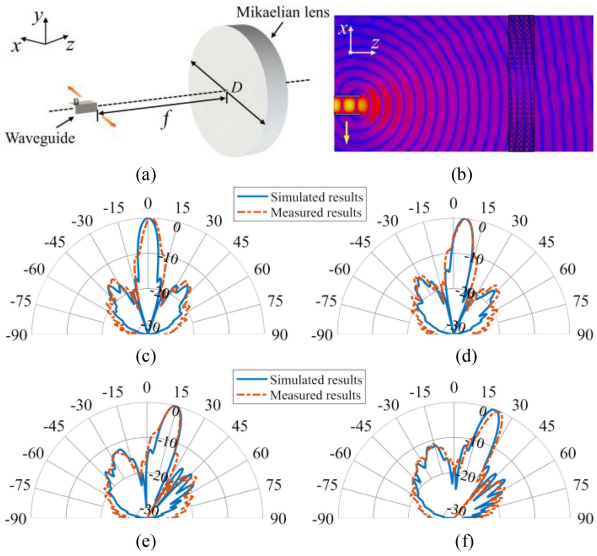

Fig. 8. (a) 3-D model. (b) Simulated 2-D electric field distribution for feeding position at $x = -30$ mm. Simulated and measured normalized H-plane radiation pattern of the lens antenna at 10 GHz for different positions. (c) $x = 0$ mm. (d) $x = -25$ mm. (e) $x = -65$ mm. (f) $x = -95$ mm.

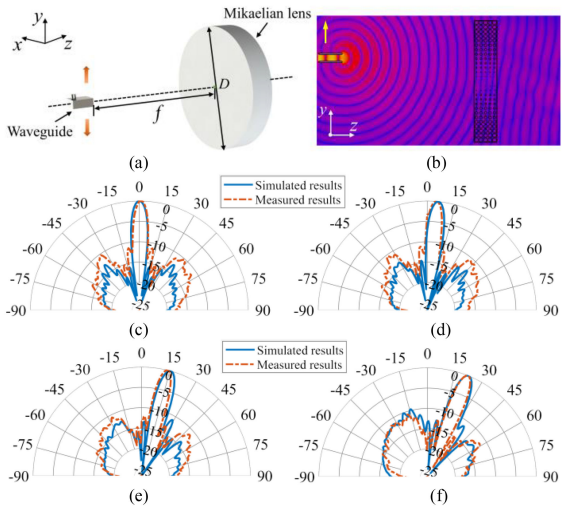

Fig. 9. (a) 3-D model. (b) Simulated 2-D electric field distribution for feeding position at $y = 30$ mm. Simulated and measured normalized H-plane radiation pattern of the lens antenna at 10 GHz for different positions. (c) $y = 30$ mm. (d) $y = -25$ mm. (e) $y = -65$ mm. (f) $y = -95$ mm.

to the lens center. Here, for the sake of brevity, the simulated and measured normalized H-plane radiation pattern of the lens antenna for different feeding positions at 10 GHz ($x = 0$, -25, -65, -95 mm) are respectively illustrated in Fig. 8(c)–(f). As the waveguide is move right along the x-axis, the high-gain radiation beam produced by lens is steered left accordingly.

The same procedure is performed to obtain the simulated and measured normalized E-plane radiation pattern of lens antenna for different feeding positions at 10 GHz ($y = 0$, -25, -65, -95 mm), as shown in Fig. 9(c)–(f). Similarly, as the waveguide is move down along y-axis, the high-gain radiation beam produced by lens is steered up accordingly, which further indicates

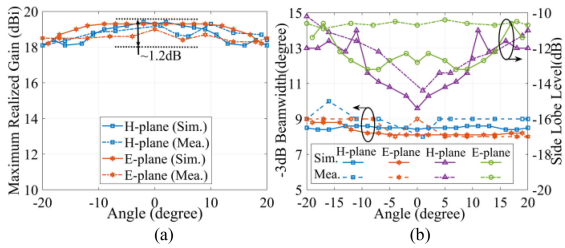

Fig. 10. (a) Simulated and measured maximum realized gain versus steering angle. (b) –3 dB beamwidth of beam and SLL in E-plane and H-plane, respectively.

the proposed lens can perform 2-D beam steering very well by moving the feeding waveguide in the focal plane.

Fig. 10(a) shows the simulated and measured peak gain versus steering angle in E-plane and H-plane, respectively. The maximum measured realized gain is 18.9 dBi. The small differences between measurement and simulation result occur due to uncertainties of measurement and limited manufacturing precision of 3-D FDM printing. Overall, the measured gain values are very close to the simulation results, indicating the good gain stability of lens with less than 1.2 dB variation among the effective beam-steering range ($\pm 20°$). In addition, the half-power beamwidth and side-lobe level (SLL) is shown in Fig. 10(b). The -3 dB beamwidth of beam with less than -10 dB SLL can be maintained well as the steering angle increases. Because an open-ended waveguide is used as the feeding source in our case, it has a certain effect on the maximum achievable gain, the SLL, steering angles and efficiency.

In our case, the efficiency of proposed lens system is mainly limited by the illumination of feeding source. Considering that the open-ended waveguide is utilized as feeding source, the aperture size of lens is much larger, resulting in low efficiency ($\sim$19.82%). It means that the proposed lens concept should be more effective if the optimization work for aperture size could be carried out. Despite the imperfections of the radiation performance with low efficiency, the simulation results are almost consistent with the measurement results, which revealing this new lens concept with unique low profile can be used in the 2-D beam-steering applications.

IV. Conclusion

An all-dielectric 2-D beam-steerable generalized Mikaelian lens using 3-D printing was proposed in this letter. Compared with conventional Luneburg, Maxwell fish-eye, and Eaton lens, the proposed lens has the unique flat shape characteristic, which provides great advantages in designing the low-profile planar lens antenna, avoiding using extremely complex conformal mapping methods. It has been demonstrated that we can achieve 2-D beam steering in both the E-and H-plane among the effective beam-steering range ($\pm 20°$) with around 18.9 dBi of realized gain with less than $\sim$1.2 dB variation and low side-lobe. This proposed lens concept could be also a potential alternative design for the existing planar GRIN lens antenna configurations, avoiding using complex conformal mapping methods.

REFERENCES

[1] H. F. Ma and T. J. Cui, "Three-dimensional broadband and broad-angle transformation-optics lens," *Nature Commun.*, vol. 1, no. 8, Nov. 2010, Art. No. 124.

[2] H. Xu, G. Wang, Z. Tao, and T. Cai, "An octave-bandwidth half Maxwell fish-eye lens antenna using three-dimensional gradient-index fractal metamaterials," *IEEE Trans. Antennas Propag.*, vol. 62, no. 9, pp. 4823–4828, Sep. 2014.

[3] G. Du, M. Liang, R. A. Sabory-Garcia, C. Liu, and H. Xin, "3-D printing implementation of an X-band Eaton lens for beam deflection," *IEEE Antennas Wireless Propag. Lett.*, vol. 15, pp. 1487–1490, 2016.

[4] A. Demetriadou and Y. Hao, "A grounded slim Luneburg lens antenna based on transformation electromagnetics," *IEEE Antennas Wireless Propag. Lett.*, vol. 10, pp. 1590–1593, 2011.

[5] M. Ebrahimpouri and O. Quevedo-Teruel, "Bespoke lenses based on quasi-conformal transformation optics technique," *IEEE Trans. Antennas Propag.,* vol. 65, no. 5, pp. 2256–2264, May 2017.

[6] A. L. Mikaelian, "Self-focusing medium with variable index of refraction," in *Progress in Optics XVII*, E. Wolf, Ed. Amsterdam, The Netherlands: North Holland, 1980.

[7] E. I. Semernya and S. P. Skobelev, "Analysis of wave focusing by axisymmetric Mikaelian lenses," *IEEE Antennas Wireless Propag. Lett.*, vol. 20, no. 2, pp. 269–273, Feb. 2021.

[8] J. Chen *et al.*, "Conformally mapped Mikaelian lens for broadband achromatic high resolution focusing," *Laser Photon. Rev.,* vol. 15, Mar. 2021, Art. no. 2000564.

[9] J. W. Yang, W. Y. Lai, H. C. Chou, and M. N. M. Kehn, "Compact Mikaelian lens synthesized by metasurfaces," *IEEE Antennas Wireless Propag. Lett.*, vol. 17, no. 3, pp. 397–400, Mar. 2018.

[10] J. Bor, B. Fuchs, O. Lafond, and M. Himdi, "Flat foam-based Mikaelian lens antenna for millimeter wave applications," in *Proc. 44th Eur. Microw. Conf.*, Rome, Italy, Oct. 2014, pp. 1640–1643.

[11] K. Nishizawa, "Principle and application on gradient index optical imaging," *Rev. Laser Eng.*, vol. 8, pp. 748–758, 1980.

[12] W. Y. Shao, H. Sato, X. T. Li, K. K. Mutai, and Q. Chen, "Perforated extensible 3-D hyperbolic secant lens antenna for directive antenna applications using additive manufacturing," *Opt. Exp.*, vol. 29, no. 12, pp. 18932–18949, Jun. 2021.